Out of Thin Air? Catalytic Oxidation of Trace Aqueous Aldehydes with Ambient Dissolved Oxygen

Euna Kim[1], Georgia B. Cardosa[1], Katarina E. Stanley[2], Travis J. Williams[3], Daniel L. McCurry[1*]

[1]Department of Civil and Environmental Engineering, University of Southern California, Los Angeles, CA 90089

[2]Department of Chemical Engineering and Materials Science, University of Southern California, Los Angeles, CA 90089

[3]Loker Hydrocarbon Research Institute and Department of Chemistry, University of Southern California, Los Angeles, CA 90089-1661

*Corresponding author phone: 213-740-0762; email: dmccurry@usc.edu

26 **TOC ART**

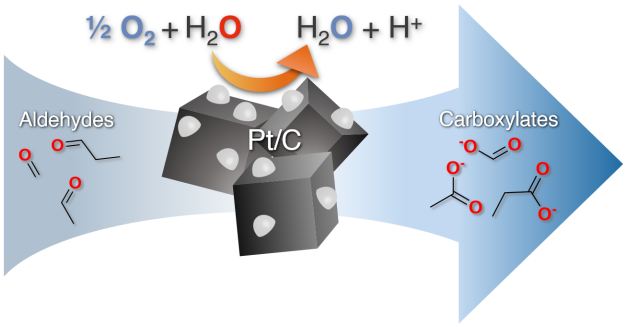

27

28

ABSTRACT

Water reuse is expanding due to increased water scarcity. Water reuse facilities treat wastewater effluent to a very high purity level, typically resulting in a product water that is essentially deionized water, often containing less than 100 µg/L organic carbon. However, recent research has found that low molecular weight aldehydes, which are toxic electrophiles, comprise a significant fraction of the final organic carbon pool in recycled wastewater in certain treatment configurations. In this manuscript, we demonstrate oxidation of trace aqueous aldehydes to their corresponding acids using a heterogeneous catalyst (5% Pt on C), with ambient dissolved oxygen serving as the terminal electron acceptor. Mass balances were essentially quantitative across a range of aldehydes, and pseudo-first order reaction kinetics are observed in batch reactors, with k_{obs} varying from 0.6 h^{-1} for acetaldehyde to 4.6 h^{-1} for hexanal, while they were low for unsaturated aldehydes. Through kinetic and isotopic labeling experiments, we demonstrate that while oxygen is essential for the reaction to proceed, it is not involved in the rate-limiting step, and the reaction appears to proceed primarily through a base-promoted beta-hydride elimination mechanism from the hydrated *gem*-diol form of the corresponding aldehyde. This is the first report we are aware of that demonstrates useful abiotic oxidation of a trace organic contaminant using dissolved oxygen.

KEYWORDS: Wastewater Recycling, Reuse, Organic Contaminants, Catalysis

SYNOPSIS

Toxic aldehydes have been found as contaminants in recycled water. This study demonstrates catalytic oxidation of aldehydes to non-toxic carboxylates with ambient dissolved oxygen.

INTRODUCTION

Increased water scarcity has motivated greater adoption of wastewater recycling to augment potable water sources.[1–3] The risk from pathogens and hazardous chemicals in wastewater is mitigated by the use of multiple treatment steps including pre-oxidation (typically with ozone or chlorine), reverse osmosis (RO), and advanced oxidation processes (AOPs).[4] Despite the high level of treatment used during wastewater recycling, recent studies have documented the presence of recalcitrant organic carbon in the final effluent, and the majority of these chemicals have not yet been fully identified.[5–7] Furthermore, some water reuse operations have considered replacing RO-based treatment trains with ozone followed by biological activated carbon (O_3/BAC) due to treatment and disposal concerns for RO concentrates,[8–11] however higher total organic carbon (TOC) concentrations are expected in the effluent of the O_3/BAC process compared to current practice (e.g., 2.5 mg/L for O_3/BAC and 0.2 mg/L for RO).[7]

Despite many studies on the low molecular weight compounds present in potable reuse product water, until recently <35% of the dissolved organic carbon in reverse osmosis permeate had been characterized.[7,12,13] One fraction, disinfection byproducts including trihalomethanes, haloacetic acids, and *N*-nitrosodimethylamine, accounts for approximately 5–10% of the TOC in the final effluent.[13] Little of the remaining unknown carbon had been identified, until a recent study demonstrated that carbonyl compounds account for 19–38% of the remaining DOC in recycled wastewater, most of which were saturated and unsaturated aldehydes.[7] These aldehydes are toxic electrophiles[14,15] and are difficult to remove with existing reverse osmosis and advanced oxidation treatment systems due to their polarity, low molecular weight, and neutral charge.[16–22]

Catalytic transformation of contaminants with environmentally-relevant, mild, and scalable conditions is a subject of considerable research interest.[23–27] Many studies using heterogeneous catalysts for environmental purposes in water have focused on the reduction of inorganic contaminants such as bromate, nitrate, and perchlorate[23,28,29] or hydrodehalogenation of halogenated organics.[29–31] Oxidative catalysis has been applied to carry out degradation of contaminants on an electrode, or on a membrane surface with the addition of strong electron acceptor such as hydrogen peroxide or persulfate.[32–37] Photocatalytic oxidative degradation of micropollutants, largely with TiO_2, has focused on oxidation by surface reactions and generation of hydroxyl radical initiated by UV irradiation.[38–42] However, catalytic oxidation of organic pollutants in water without electrochemistry, addition of electron acceptors, or photochemistry, each of which challenge the potential scalability of the respective methods, has not been demonstrated to the best of our knowledge.

In this study, we sought to extend the concept of "Catalytic Converters for Water Treatment"[27] from reductive treatment of oxyanions to oxidation of organic pollutants, by oxidizing contaminants with dissolved molecular oxygen as the terminal electron acceptor. We first identified a catalyst in the organic synthesis literature reported to be capable of oxidizing aqueous alcohols and aldehydes to their corresponding acids in the presence of dissolved oxygen and aimed to identify its substrate scope in batch experiments. We determined kinetic parameters for oxidation of a range of low molecular weight aldehydes, aimed to elucidate the reaction mechanism, in particular the role of dissolved oxygen, and to demonstrate preliminary effectiveness in a flow-through column reactor more closely resembling deployment in full-scale water treatment. This study takes a first step toward oxidation of trace aldehyde compounds in

final recycled water effluent to generally non-toxic organic acids, using heterogeneous catalysts and ambient molecular oxygen.

MATERIALS AND METHODS

Materials and Reagents. Chemical suppliers and purities are listed in Text S1.

Catalyst Characterization. The morphology of the catalyst supporter was observed by scanning electron microscope (SEM) using Thermo Scientific Helios G4 PFIB UXe, and the size distribution of catalyst particles was measured by using dynamic light scattering (DLS) with a Zetasizer Ultra (Malvern Instruments Ltd., UK). A 4-mL of 0.4 g/L suspension of Pt/C was prepared in Milli-Q water and transferred to a polystryrol/polystyrene cuvette for analysis. The light scattering was measured after equilibrating samples at 25 °C for 120 seconds with a refractive index of 1.63 and an absorption of 0.001. The size and dispersion of the platinum supported on the carbon was characterized by measuring scanning transmission electron microscopy (STEM) and transmission electron microscopy (TEM) using JEOL 2100F at 200 kV with high angle annular dark field detector.

Batch Experiments to Determine Aldehyde Oxidation Kinetics. Batch experiments were performed in 100 mL glass syringes to avoid creating headspace while sampling periodically, because several target compounds were semi-volatile and mass balance was not conserved in preliminary tests in open reactors. Within the syringes, 40 mg of heterogeneous 5% Pt on C catalyst particles were suspended in 99 mL of 10 mM buffer solution adjusted to pH 4–12: citrate for pH 4, 5 and 6, phosphate for pH 7, 8 and 12, and carbonate for pH 9, 10 and 11. After adding

a magnetic stir bar, the syringe was fitted tightly with a glass plunger and secured to a stir plate. Once the catalyst was dispersed homogeneously in the syringe, 1 mL of concentrated aqueous aldehyde solution was injected to initiate the reaction. Aliquots of 4.5 mL were withdrawn periodically and filtered with a syringe filter (0.2 μm, PTFE).

^{18}O-labeled Water Experiments. Batch oxidation reactions were conducted in ^{18}O-labeled water ($H_2{}^{18}O$) to differentiate water-derived oxygen atoms in the reaction products from O_2-derived oxygen atoms. In 2 mL HPLC vials, 1.6 mg of the catalyst was added along with 400 μL of ^{18}O-labeled water containing 97 atom % ^{18}O. To initiate the reaction, 0.36 μL of pure butyraldehyde or 0.41 μL of pure benzaldehyde ($[aldehyde]_0$ = 10 mM) was added to the vials along with a small stir bar. The solutions were then stirred for six hours and filtered through a 0.2 μm syringe filter before analysis. The hydration equilibrium of butyraldehyde was evaluated with 5% v/v of ^{18}O-labeled water ($H_2{}^{18}O$) in 2 mL HPLC vials, and the m/z values were acquired by using GC/MS/MS (Agilent 7890B/7010) at two reaction time intervals, 2 h and 5 d.

Flow-through Column Reactor Experiments. A small-scale column test was conducted to determine the feasibility of aldehyde oxidation by Pt/C catalysts in a flow-through configuration. The borosilicate glass column had a length of 70 mm and an inner diameter of 5.6 mm for a total bed volume of 1.72 cm^3. The column was packed with a heterogenous mixture of 40 mg of platinum on carbon dispersed in 3 g of Ottawa sand (to increase hydraulic conductivity) and was plugged on each end with glass fiber. A 100 μM formaldehyde solution was pumped from an amber borosilicate bottle with a peristaltic pump at a flow rate of 0.256 mL/min, which led to an empty bed contact time (EBCT) of 6.7 minutes as shown below (eq. (1)):

$$EBCT = \frac{Bed\ volume\ (mL)}{Flow\ rate\ (mL/min)} = \frac{1.72\ mL}{0.256\ mL/min} = 6.7\ min \quad (1)$$

Reactant and Product Analysis. Depending on the reaction parameters, experiments were conducted at two different ranges of initial concentration. When the initial concentration of reactants was over 100 μM, the analytes (aldehydes and acid products) were analyzed via high pressure liquid chromatography (HPLC; Agilent 1260). Analytes were separated on an Aminex HPX-87H (300 mm × 7.8 mm × 9 μm) column without pretreatment. The mobile phase (30% acetonitrile and 70% aqueous sulfuric acid (20 mM)) was pumped through the column at 0.5 mL/min at 60 °C with a sample injection volume of 100 µL. The analytes were detected by a photodiode array (Agilent 1260) at 206 nm for aldehydes and 282 nm for carboxylic acids.

For initial reactant concentrations below 25 µM, aldehydes were derivatized by adding 20 µL of a 3 mg/mL 2,4-dinitrophenylhydrazine solution and 40 µL of 1 M citrate buffer solution adjusted to pH 3 to a 1 mL of sample aliquot.[43] After heating the solution at 50 °C for two hours, the aldehyde derivatizes were separated via HPLC (Agilent 1290 or Agilent 1260) on a Kinetex Biphenyl column (100 mm × 4.6 mm × 2.6 µm). The mobile phase consisted of an organic channel (50:50 methanol:ethanol) which increased from an initial 60% to 75% over 10 minutes at a constant flowrate of 1.3 mL/min at 40 °C, with the remainder of the mobile phase consisting of Milli-Q (Millipore Advantage A10) water. The separated compounds were detected by either high-resolution mass spectrometry (Agilent 6560 ion mobility quadrupole time-of-flight [LC-IM-QTOF]) with negative mode electrospray ionization (details provided in Table S1; all mass errors <3 ppm), or with a UV/visible photodiode array detector (Agilent 1260) at 360 nm for derivatized saturated aldehydes and at 382 nm for derivatized crotonaldehyde. For product

analysis, carboxylic acids were separated by a Dionex IonPac AS11-HC column (250 mm × 2 mm × 9 μm) in an aqueous mobile phase of KOH increasing from 1 mM to 9 mM over 8 minutes and measured via ion chromatography (Dionex ICS-2100) with DS6 heated conductivity cell. Platinum was quantified in column experiment permeate via inductively-coupled plasma mass spectrometry (ICP-MS; Agilent 8900).

When conducting ^{18}O-labeled water experiments, butyric acid and benzoic acid were separated by an Agilent Extend-C18 column (50 mm × 2.1 mm × 1.8 μm) in an isocratic mobile phase of 30% acetonitrile and 70% aqueous formic acid (0.1%) at a constant flow rate of 0.5 mL/min at 40 °C, and detected by high-resolution MS (Agilent 6560) in positive mode. Mass spectrometry details are provided in Table S2. All measured mass errors were < 10 ppm. For butyraldehyde measurement, 1 mL aqueous samples were placed in 4 mL vials, and 0.4 g of Na_2SO_4 was added. After adding 1 mL of dichloromethane, the vials were vigorously shaken for 2 minutes, and the organic solvent phase was transferred to a 2 mL of HPLC vial. Butyraldehyde was analyzed via gas chromatography/triple quadrupole mass spectrometry (GC/MS/MS) (Agilent 7890B/7010, Santa Clara, CA) with a DB-1701 column (60 m × 0.25 mm × 0.25 μm) Measurement details are provided in Text S2 and Table S3.

Dissolved Oxygen Measurement. Dissolved oxygen concentrations were measured using a modified Winkler method.[44] To minimize headspace, 2 mL of sample was injected into a 2 mL HPLC vial. 20 μL of 3.55 M manganese sulfate monohydrate was then added, followed by 20 μL of a solution composed of 8 M sodium hydroxide, 3.34 M potassium iodide, and 0.15 M sodium azide. Finally, 20 μL of pure sulfuric acid was added to dissolve the precipitate. Dissolved oxygen was quantified as iodine (produced at a 2:1 stoichiometric ratio) by titrating

with 25 mM sodium thiosulfate and 10 mM sodium hydroxide; starch was added midway through the experiment to visually indicate the completion of the titration as the dark blue solution became transparent. Further details are provided in Text S3.

Statistical Analysis. Experimental results were statistically analyzed using GraphPad Prism 9, with a simple linear regression model and a sum-of-squares F test with 95% confidence intervals. The slopes of logarithm-transformed data sets were compared by analysis of variance (ANOVA).

RESULTS AND DISCUSSION

Catalyst Characterization. Catalyst particles were rough, consistent with an activated carbon supporter (Figure S1, panels a-d), with a mean particle size of 226 nm and a standard deviation was 31 nm (Figure S2). Platinum sites were approximately uniformly dispersed (Figure S3, panels a-c), with a size of less than 5 nm on the carbon surface (Figure S3, panel d).

Aldehyde Oxidation Reaction Rate Order and Rate Constants. Based on previous research identifying the presence of certain toxic aldehydes in the final recycled water effluent,[7] six saturated aldehydes and one unsaturated aldehyde were chosen as oxidation targets: formaldehyde, acetaldehyde, propionaldehyde, butyraldehyde, pentanal, hexanal and crotonaldehyde. Initial aldehyde oxidation experiments were performed with relatively low initial aldehyde concentrations to ensure approximately constant dissolved oxygen concentrations for determination of rate constants. Aldehyde concentrations decreased while corresponding acid product concentrations increased, following apparent first-order kinetics (representative dataset in Figure 1a; complete set in Figure S4; log-transformed data to obtain

rate constants in Figure S5). Mass balances were approximately complete except for with hexanal (Figure S4, panel e), which is discussed below. The nearly 100% mass balance indicates that aldehyde oxidation by Pt/C/O_2 produces the corresponding acids as an exclusive product under the evaluated experimental conditions.

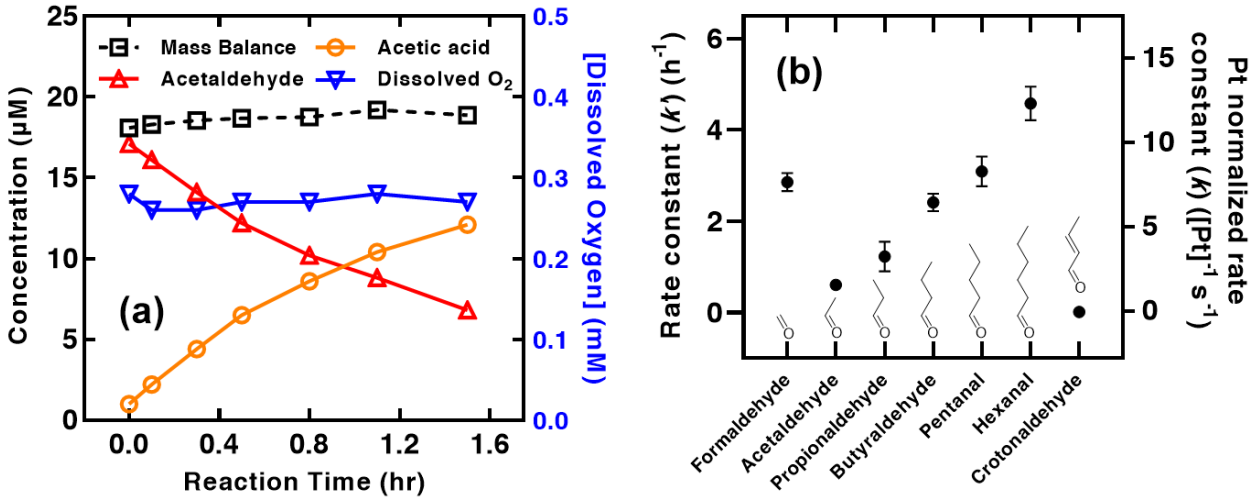

Figure 1. (a) Representative reaction profile for acetaldehyde oxidation including acetaldehyde, acetic acid, and dissolved oxygen concentrations, and mass balance (sum of aldehyde and acid). (b) Aldehyde oxidation first-order rate constants (h^{-1}) and rate constants normalized by platinum atom concentration ($[Pt]^{-1}$ s^{-1}). Error bars indicate the standard deviation of the rate constants determined by linear regression of replicate values. Experimental values without error bars indicate that the error bars are smaller than the data marker. Experimental conditions: 40 mg/100 mL of Pt/C catalyst, 20 μM nominal initial aldehyde concentration, pH 7, 10 mM phosphate buffer, T = 24 ± 0.5 °C.

For saturated aldehydes, observed first-order oxidation rate constants (k_{obs}) increased as the length of the carbon chain increased: 0.61 ± 0.06 h^{-1} for acetaldehyde, 1.23 ± 0.32 h^{-1} for propionaldehyde, 2.42 ± 0.19 h^{-1} for butyraldehyde, 3.09 ± 0.32 h^{-1} for pentanal, and 4.58 h^{-1} ± 0.37 h^{-1} for hexanal. Corresponding rate constants normalized by molar concentration of platinum, as previously treated for other noble metal catalysts,[23] ranged from 1.7 to 12.4 ($[Pt]^{-1}$ s^{-1}), and are provided on the secondary y-axis of Figure 1b. When oxidizing hexanal, the hexanal

concentration in the first sample was measured to be less than half of the initial concentration, resulting in a poor mass balance at that time point (Figure S4, panel e). As the reaction progressed, the mass balance recovered as the concentration of the product increased and eventually plateaued. Because hexanal is relatively hydrophobic (e.g., K_{ow} = 1.80 for hexanal; K_{ow} = 0.82 for butyraldehyde[45]) the hexanal rapidly absorbed to the syringe filter used for separating the catalyst and aqueous solution, resulting in an apparent rapid decrease in aqueous concentration. As sorbed hexanal was oxidized to produce hexanoic acid, the mass balance recovered. To account for the phenomenon, the reaction rate of hexanal oxidation was calculated by using the concentration of hexanoic acid assuming a single rate-limiting step (derivation of integrated rate law provided in Text S4).

Longer chain saturated aldehydes generally reacted faster, with observed first order rate constants increasing monotonically from acetaldehyde to hexanal, potentially suggesting a rate-limiting mass transfer step aided by the higher hydrophobicity of the longer aldehydes. However, formaldehyde was oxidized approximately five times faster than acetaldehyde with an observed rate constant of 2.86 ± 0.20 h^{-1}. Crotonaldehyde, which contains the same number of carbons as butyraldehyde but is unsaturated at the 2-position, reacted with the slowest observed rate constant of 0.0102 h^{-1} ± 0.0012 h^{-1}. We sought explanations for the apparent relationship between structure and reactivity for oxidation of aldehydes by $Pt/C/O_2$, by probing the reaction mechanism, as discussed below.

First, to determine the reaction rate order of aldehydes in the rate-limiting step, initial rate kinetics experiments were performed with acetaldehyde. Acetic acid concentration was monitored during approximately the first 10% of the reaction, during which the concentrations of acetaldehyde and dissolved oxygen changed negligibly. These reactions were performed at three

different acetaldehyde concentrations, and logarithmic transformation of a generic rate law (Text S5), gives an equation which can be plotted to give the rate order as the slope of a linear regression (Figure S5). In this case, the slope was statistically significantly indistinguishable from 1.0 ($p = 0.5966$), indicating that the rate-limiting step of the reaction is first-order in aldehyde concentration (Figure S6). This observation is consistent with the results of experiments performed at low initial concentration, in which the reaction appeared to remain first order, even at concentrations below 1 μM, close to the aldehyde concentration observed in the product water of some reuse facilities (Figure S5).

Next, we evaluated the rate order of the catalyst in the reaction. While catalytic reactions are often zero-order in catalyst (if the catalyst is saturated), a first-order rate dependence on catalyst dose may occur if the reactants do not saturate the catalyst. To determine the reaction rate order for the available Pt sites, initial rate experiments were conducted at different catalyst loadings, analogously to the aldehyde rate order determination above. The reaction order for available Pt sites also followed first-order kinetics, with a slope statistically indistinguishable from 1.0 ($p = 0.2139$) (Figure S7).

Role of Dissolved Oxygen in Catalytic Oxidation of Aldehydes. To confirm that oxygen is required for the reaction to proceed (e.g., ruling out evolution of hydrogen gas or Cannizzaro disproportion as the mechanism of oxidation, that are known to occur in late-metal catalyzed alcohol-to-carboxylate oxidation[46]), superstoichiometric initial acetaldehyde concentrations were applied in a closed system containing the catalyst, to deliberately deplete dissolved oxygen and observe whether the reaction continued in the absence of oxygen. Once oxygen was depleted, aldehyde oxidation ceased (Figure 2a). In a second experiment performed under similar conditions but with a much lower propionaldehyde concentration, once the aldehyde oxidation

was complete, the dissolved oxygen concentration remained approximately constant (Figure 2b), indicating that the catalyst does not consume oxygen on its own. Both experiments suggest that molecular oxygen is essential for oxidizing aldehydes with the Pt/C catalyst. To further verify that oxygen is essential for the reaction to occur, a batch experiment was performed butyraldehyde and the catalyst in N_2-purged solution to minimize the dissolved oxygen concentration, and the reaction rate slowed dramatically (0.17 ± 0.08 h-1 versus 2.42 ± 0.13 h-1 with ambient dissolved oxygen levels) (Figure S8). In a final experiment at an intermediate starting aldehyde concentration, the aldehyde oxidation rate remained approximately constant, continuing to follow first-order kinetics, while oxygen concentration was decreasing (Figure S9), suggesting that while oxygen is essential for the reaction to proceed, the reaction rate does not depend on the dissolved oxygen concentration, as further investigated below.

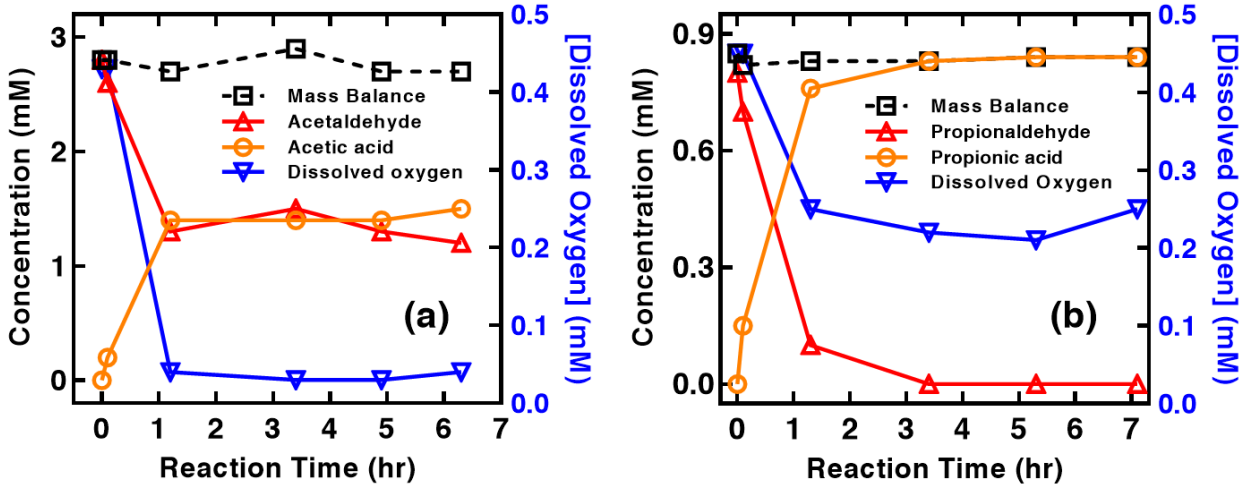

Figure 2. Reaction profiles for aldehyde oxidation including aldehyde, carboxylic acid, and dissolved oxygen concentrations, and mass balance (sum of aldehyde and acid concentrations). Experimental conditions: 40 mg/100 mL of Pt/C catalyst, initial concentrations of 3 mM and 1 mM, pH 7, 10 mM phosphate buffer, T = 24 ± 0.5 °C. (a) Acetaldehyde, (b) Propionaldehyde.

Puzzlingly, in both oxygen consumption experiments, the oxygen consumption was approximately one fourth of the concentration of aldehyde oxidized, i.e., 4:1 aldehyde:O_2 stoichiometry, where a 2:1 ratio is expected to mediate a 2 e- oxidation with a 4 e- oxidant. One possible explanation is that in a batch reactor, the catalyst is retaining electronic holes, either in the carbon support or in the form of high-valent Pt, that remain from air exposure prior to introduction to the reaction.

To test directly whether oxygen is involved in the rate-determining step of aldehyde oxidation, initial rate kinetics experiments were performed to determine the reaction rate order in oxygen. Formation of acetic acid during aldehyde oxidation was monitored during approximately the first 10% of conversion, during which the concentrations of acetaldehyde and dissolved oxygen change negligibly. These reactions were performed at three different dissolved oxygen concentrations (Figure 3, panels (a)-(c)) and analyzed as described previously to determine the rate order in oxygen, which was statistically indistinguishable from zero ($p = 0.4079$) (Figure 3d), indicating that dissolved oxygen is not involved in the rate-limiting step of the reaction.

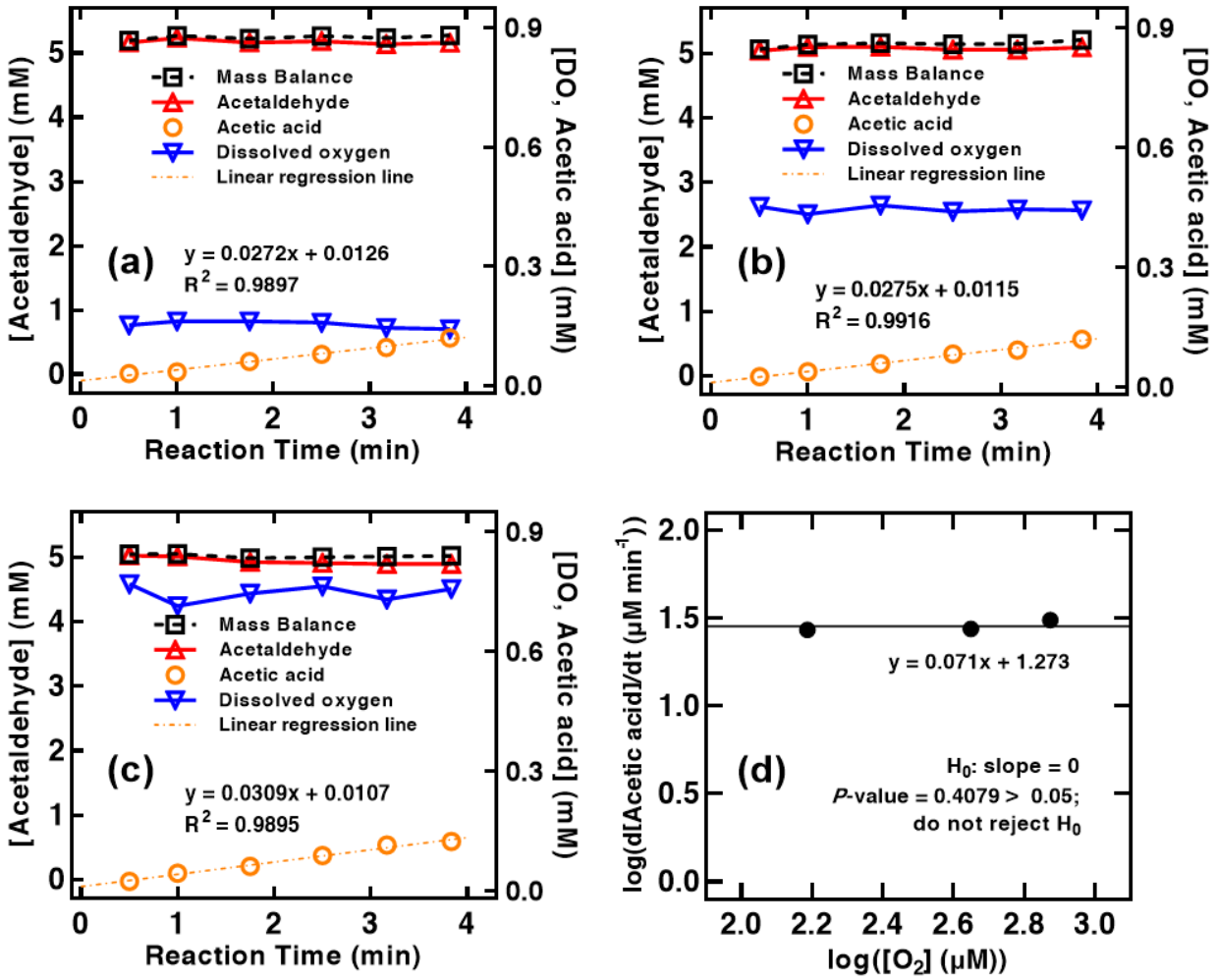

Figure 3. Aldehyde oxidation to respective products under initial rate conditions (at three different fixed oxygen concentrations [panels (a)-(c)]) to determine reaction rate order in oxygen [panel (d)]. Reactions were performed at pH 7 in 10 mM phosphate buffer with 400 mg/L of Pt/C catalyst, temperature: 24 ± 0.5 °C.

Last, to evaluate whether reactive oxidative species (ROS), such as hydroxyl radical and singlet oxygen, are involved in the reaction pathway, kinetics experiments were conducted in the presence of ROS scavengers: 1 mM of *tert*-butanol for scavenging hydroxyl radical, and 1 mM of 2-furoic acid for scavenging singlet oxygen, respectively. Furoic acid was chosen over furfuryl alcohol[47] to avoid scavenger oxidation by the catalyst, which is capable of oxidizing primary alcohols.[48] Butyraldehyde oxidation was not slowed by the presence of *t*-butanol (p =

0.3552), ruling out a role for hydroxyl radical (Figure S10). 2-furoic acid slowed the butyraldehyde oxidation rate slightly but statistically significantly (from 0.57 h^{-1} to 0.40 h^{-1}; $p = 0.0021$). However, the slight decline suggests that singlet oxygen generation is not the primary oxidation pathway, and it is possible that the addition of the 2-furoic acid scavenger to the system affected the reaction rate in some other way, e.g., by blocking catalyst active sites.

Aldehyde Oxidation Mechanism by Pt/C in Aqueous Solution. To begin probing the reaction mechanism, acetaldehyde oxidation experiments were conducted at a range of pH values (4 - 12) different buffer concentrations to determine whether the rate-limiting step might be acid- or base-catalyzed. As pH increased, the observed oxidation rate of aldehydes increased from 0.14 ± 0.06 h^{-1} at pH 4 to 7.76 ± 0.26 h^{-1} at pH 12 (Figure S11 and S12). However, the reaction rate was not significantly affected by buffer concentration ($p = 0.7422$) (Figure S13). These experimental results suggest the intuitive conclusion that aldehyde oxidation is base-promoted but not buffer-catalyzed. Reaction rate dependence on ionic strength was evaluated by varying ionic strength with NaCl and pure Milli-Q water while maintaining otherwise identical conditions, and no significant relationship was found in different NaCl concentrations ($p = 0.5815$) (Figure S14), but the formaldehyde oxidation rate in pure water was calculated as 11.2 h^{-1} (Figure S15), which was considerably faster than the reaction rate acquired with buffered solution at nearly the same pH (4.95 h^{-1} at pH 7).

To further investigate the mechanism, butyraldehyde and benzaldehyde, representatives of aliphatic and aromatic aldehydes respectively, were oxidized by Pt/C in ^{18}O-labeled water to differentiate oxygen atoms originating from dissolved oxygen ($^{16}O_2$) from those derived from water ($H_2{}^{18}O$). The majority of the carboxylic acid products (85.0% of butyric acid and 85.9% of

benzoic acid) were doubly-labeled with two ^{18}O atoms, meaning that both oxygens were derived from water (Figure 4). 15.0% of butyric acid and 13.0% of benzoic acid are labeled with one ^{18}O atom and one ^{16}O atom, suggesting that one oxygen atom from $H_2{}^{16}O$, the product of Pt-catalyzed $^{16}O_2$ reduction, incorporated into the carboxylic acid product. While it might not fully explain 14% ^{16}O incorporation, ^{18}O atom exchange with ^{16}O silicates in the glass may have contributed. Regardless, only a small portion of unlabeled acids was found, indicating that dissolved oxygen did not react directly with dissolved organics in this reaction. In the gas phase, platinum is known to dissociate molecular oxygen into two oxygen atoms that incorporate into the aldehyde to form a carboxylate on the surface,[49–52] but this reaction is inconsistent with our observation on the origin of the oxygen atoms in the product.

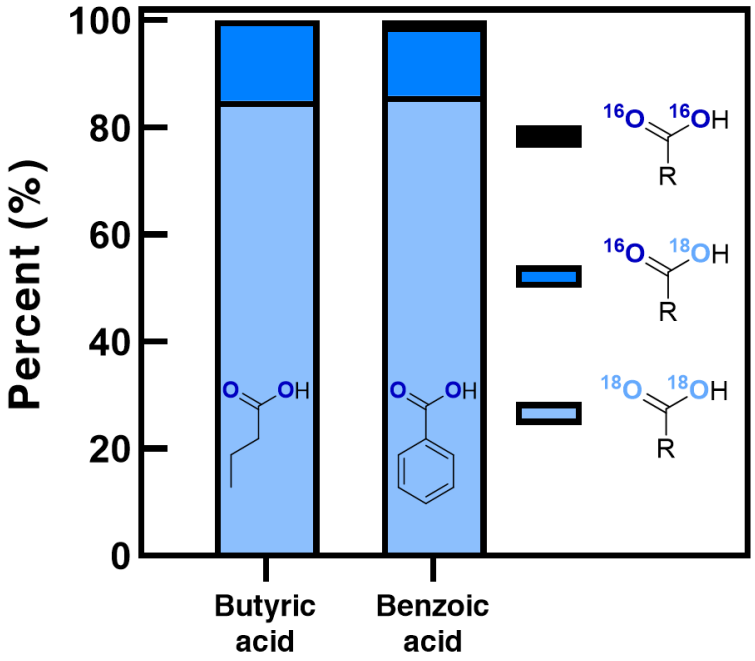

Figure 4. Isotopic distribution of acid products from butyraldehyde and benzaldehyde oxidation. Reactions were performed in 97 atom % ^{18}O-labeled water with 4 g/L of Pt/C catalyst for 6 hours, temperature: 24 ± 0.5 °C.

Aldehydes in aqueous solution rapidly hydrate to the corresponding *gem*-diol in a reversible equilibrium (Scheme 1), replacing the oxygen atom in the carbonyl group with oxygen from water. The replacement of oxygen atoms in aldehydes by water was confirmed by measuring m/z of butyraldehyde in 1 mL of 5% v/v of ^{18}O-labeled heavy water ($H_2{}^{18}O$) at two reaction time intervals, 2 hours and 5 days. GC/MS/MS analysis indicated that the m/z distribution of ^{18}O-labeled butyraldehyde ($C_4H_8{}^{18}O$) relative to total butyraldehyde was 5% at both reaction times (Figure S16), indicating that aldehyde had fully exchanged its oxygen atom with water within 2h. The hydration equilibrium constant between the two species (K_{hyd} = $RCH(OH)_2/RCHO$) is a function of chemical structure, generally decreasing for primary aldehydes as chain length increases (2000 for formaldehyde, 1.20 for acetaldehyde, 0.85 for propionaldehyde, 0.60 for butyraldehyde, 0.55 for pentanal, 0.50 for hexanal, 1.13 for crotonaldehyde).[53,54] In contrast, aromatic aldehydes such as benzaldehyde are predominantly present as the aldehydic form (K_{hyd} = 0.008).[55] Regardless of the value of the equilibrium constant, all aldehydes dissolved in ^{18}O-labeled water with sufficient time to reach equilibrium will have fully-labeled oxygens in both forms: aldehydes with one ^{18}O atom and *gem*-diols with two ^{18}O atoms.

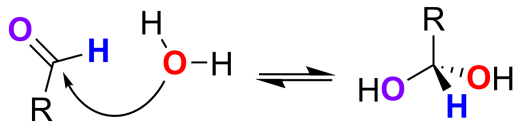

Scheme 1: Aldehyde equilibrium with hydrated *gem*-diol.

Given that aldehydes exist in aqueous solution as both the free carbonyl and the *gem*-diol, we anticipated that each form must either proceed through a pre-equilibrium scenario or through

a different reaction mechanism. We find the latter unlikely, because equal isotope ratios of the products of butyraldehyde (large K_{hyd}) and benzaldehyde (small K_{hyd}) imply that $^{16}O_2$, or an R^{16}OS therefrom, is not reacting directly, as might be proposed for transformation of the free carbonyl form of the aldehyde. Moreover, alcohol oxidation on Group 8-10 metal catalysts in aqueous solution is known to proceed through a dehydrogenation mechanism.[56–59] A similar mechanism explains oxidation of primary alcohols to carboxylic acids (or esters), via a Tishchenko-like pathway involving hydration (or alcoholysis) of the intermediate aldehyde.[46] A mechanism proceeding through the diol is also consistent with kinetic observations: 1) the reaction rate of formaldehyde, which is overwhelmingly hydrated, is five times faster than acetaldehyde which is hydrated to a lesser degree at equilibrium. 2) benzaldehyde, despite a similar hydrophobicity (K_{ow} = 1.71) to hexanal (K_{ow} = 1.80),[45] is oxidized much more slowly (0.19 ± 0.14 h^{-1} (Figure S17) compared to 4.58 ± 0.37 h^{-1})). This is consistent with the reaction proceeding primarily though the *gem*-diol, and the extent of hydration driving reactivity, as benzaldehyde is present primarily as the aldehyde (K_{hyd} = 0.008),[55] while hexanal is hydrated to a greater extent (K_{hyd} = 0.50).[53]

To further understand the rate-limiting step of the reaction, aldehyde oxidation experiments were conducted at different temperatures, and the reaction rates were calculated to determine activation parameters. Transition state enthalpy ($\Delta H^{\ddagger}$), entropy ($\Delta S^{\ddagger}$), and activation energy were calculated using Eyring and Arrhenius plots (Table 1, Figure S18).[60] Negative values of $\Delta S^{\ddagger}$ suggest that two molecules are combining in the rate-limiting step (i.e., it is a bimolecular reaction).[61]

Table 1. Calculated activation terms from data in Figure S18. The experiments were conducted at 10, 25 and 40 °C in 10 mM pH 7 phosphate buffer with 400 mg/L of Pt/C catalyst.

	Formaldehyde	Acetaldehyde	Propionaldehyde

$\Delta H^{\ddagger}$ (kJ/mol)	22.18 ± 3.81	19.77 ± 5.53	26.54 ± 5.98
$\Delta S^{\ddagger}$ (kJ/mol-K)	-0.23 ± 0.01	-0.24 ± 0.02	-0.22 ± 0.02
Ea (kJ/mol)	24.63	22.22	28.97

412

413

414 Based on the results from Figures 3, S11, and 4, and Table 1, two possible reaction
415 pathways of aldehyde oxidation are suggested in Scheme 2 and Scheme S1. Each incorporates
416 oxygen from either H_2O (major pathway) or O_2 (minor pathway) into the carboxylate, respectively
417 involving a *β*-hydride elimination from *gem*-diol or platinum insertion into aldehyde C–H bond.
418 For the first pathway, we suspect that platinum binds a hydroxyl group of the *gem*-diol. The
419 aldehyde C–H group is then cleaved by *β*-hydride elimination to form the product carboxylate and
420 an intermediate platinum hydride. The latter is oxidized by O_2 in a subsequent step. We suspect
421 that if a second, direct aldehyde oxidation pathway occurs, it involves aldehyde C-H insertion as
422 shown in Scheme S1. The apparent rate-limiting step is consistent with the slow reaction rates of
423 crotonaldehyde and benzaldehyde in which the compound contains multiple carbons with low
424 electron density, potentially serving as alternative targets for the Lewis acid sites of platinum rather
425 exclusively reacting with the gem-diol.[14,62] The significantly faster reaction rate for formaldehyde
426 relative to acetaldehyde is also consistent with the reaction proceeding through the gem-diol form,
427 as almost all formaldehyde exists in aqueous solution as the hydrated geminal diol form.

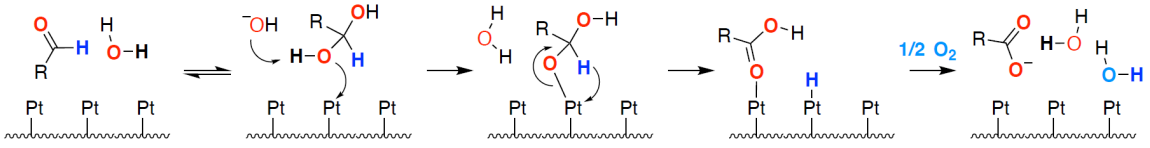

428

429 **Scheme 2**. Proposed aldehyde oxidation reaction pathway through *β*-hydride elimination.

430

Aldehyde Oxidation in a Flow-through Column. To make a preliminary evaluation of the ability of the $Pt/C/O_2$ system to serve as a flow-through "catalytic convertor" for oxidizing aldehydes in recycled wastewater, a column experiment was performed continuously pumping 100 μM formaldehyde, which was the most abundant aldehyde found in RO permeate at reuse plants,[7] through glass tubes filled with homogenously mixed Pt/C catalyst and Ottawa sand. Formaldehyde concentrations in the aliquots collected from the outlet of the glass tubes indicated that the initial conversion rate of the formaldehyde was > 99% at the catalyst loading and EBCT evaluated (23 mg/cm^3 and 6.7 min), and remained at 90% after treating 2162 bed volumes, corresponding to oxidation of 6.4 mmol C/g-Pt^{-1} (24.8 mol-formaldehyde mol-Pt^{-1}) (Figure 5). At the end of the experiment after 6239 bed volumes, the conversion rate was 68.5%. The consistent mass balance suggests that oxidation to formic acid was the dominant removal mechanism of formaldehyde. The incomplete mass balance relative to nominal initial formaldehyde concentration may be attributable to loss of formaldehyde, which is semi-volatile, to the atmosphere during feed solution preparation. In a second column experiment, platinum concentration and particle size distribution were measured in column permeate by ICP-MS and DLS over 1600 bed volumes, to assess whether catalyst loss may explain declining reactivity. The permeate contained a small amount of Pt (~1 ppb) (Figure S19), and DLS measurements found particles in the permeate with an average size of 226 nm, consistent with our prior measurements of catalyst particle size. These results suggest that particle escape, rather than Pt leaching or loss of catalyst potency, may explain declining reactivity. Future work should evaluate the possibility of better retaining the Pt/C particles, and possibly regenerating catalysts. Finally, the dissolved oxygen concentration at the outlet of the column with Pt/C catalyst was

consistently lower than the control column filled only with the sand (Figure S20), confirming that oxygen is consumed during the reaction in the column.

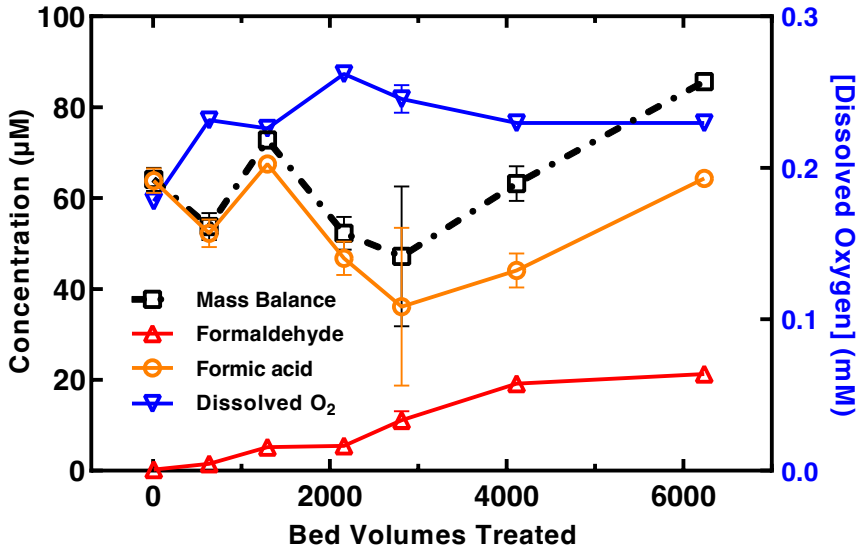

Figure 5. Reaction profile of flow-through reactor for aldehyde oxidation including formaldehyde, formic acid, and dissolved oxygen concentrations and mass balance. Experimental conditions: 40 mg of Pt/C catalyst mixed with 3 g of Ottawa sand, pH 7 in 10 mM phosphate buffer, temperature: 24 ± 0.5 °C.

Implications. Platinum and palladium catalysts, while costly, are present at gram scale in virtually every truck and automobile in the United States in a catalytic converter, the function of which is to fully oxidize dilute, partially-oxidized organic compounds, especially CO, in a fluid containing oxygen. A recent article used the term "Catalytic Converters for Water Treatment" somewhat figuratively to refer to oxyanion reduction in water using rare metal catalysts and an electron source. Herein, we have taken the first step toward applying this term literally and demonstrated oxidative catalytic water treatment with noble metal catalysts and ambient molecular oxygen. Future work should examine catalyst robustness in dirtier matrices, regeneration of spent catalysts, whether similar reactivity to Pt could be obtained with cheaper materials (e.g., Ni, Cu), whether

the poor reactivity for unsaturated aldehydes could be improved, and whether practical scale-up is achievable in a flow-through passive treatment step at the end of a reuse treatment train.

Acknowledgements: E.K. was partially supported by a USC Provost Fellowship. We acknowledge additional funding from the National Science Foundation (Award Nos. CBET-1944810 (D.L.M.) and CHE-1856395 (T.J.W.)).

Supporting Information: The Supporting Information is available free of charge on the ACS Publications website at DOI:

Supporting Information: Chemical suppliers and purities; analytical details; additional kinetics data; Eyring and Arrhenius plots.

References

(1) Khan, S. J. Potable Reuse of Water. *Environ. Sci. Water Res. Technol.* **2015**, *1* (5), 550–553. https://doi.org/10.1039/c5ew90021b.

(2) National Research Council. *Water Reuse: Potential for Expanding the Nation's Water Supply through Reuse of Municipal Wastewater*; National Academies Press, 2012. https://doi.org/10.17226/13303.

(3) Sedlak, D. L. *Water 4.0: The Past, Present, and Future of the World's Most Vital Resource*; New Haven: Yale University Press, 2014.

(4) Marron, E. L.; Mitch, W. A.; Gunten, U. Von; Sedlak, D. L. A Tale of Two Treatments: The Multiple Barrier Approach to Removing Chemical Contaminants during Potable

Water Reuse. *Acc. Chem. Res.* **2019**, *52* (3), 615–622. https://doi.org/10.1021/acs.accounts.8b00612.

(5) Abbott. 2020 Annual Report. *Mitsubishi Annu. Rep.* **2020**, No. March, 90.

(6) Kali, S.; Khan, M.; Ghaffar, M. S.; Rasheed, S.; Waseem, A.; Iqbal, M. M.; Bilal khan Niazi, M.; Zafar, M. I. Occurrence, Influencing Factors, Toxicity, Regulations, and Abatement Approaches for Disinfection by-Products in Chlorinated Drinking Water: A Comprehensive Review. *Environ. Pollut.* **2021**, *281*, 116950. https://doi.org/10.1016/j.envpol.2021.116950.

(7) Marron, E. L.; Prasse, C.; Buren, J. Van; Sedlak, D. L. Formation and Fate of Carbonyls in Potable Water Reuse Systems. *Environ. Sci. Technol.* **2020**, *54* (17), 10895–10903. https://doi.org/10.1021/acs.est.0c02793.

(8) Joo, S. H.; Tansel, B. Novel Technologies for Reverse Osmosis Concentrate Treatment: A Review. *J. Environ. Manage.* **2015**, *150*, 322–335. https://doi.org/10.1016/j.jenvman.2014.10.027.

(9) Gerrity, D.; Owens-Bennett, E.; Venezia, T.; Stanford, B. D.; Plumlee, M. H.; Debroux, J.; Trussell, R. S. Applicability of Ozone and Biological Activated Carbon for Potable Reuse. *Ozone Sci. Eng.* **2014**, *36* (2), 123–137. https://doi.org/10.1080/01919512.2013.866886.

(10) Hooper, J.; Funk, D.; Bell, K.; Noibi, M.; Vickstrom, K.; Schulz, C.; Machek, E.; Huang, C. H. Pilot Testing of Direct and Indirect Potable Water Reuse Using Multi-Stage Ozone-Biofiltration without Reverse Osmosis. *Water Res.* **2020**, *169*, 115178. https://doi.org/10.1016/j.watres.2019.115178.

(11) Gerrity, D.; Snyder, S. Review of Ozone for Water Reuse Applications: Toxicity,

Regulations, and Trace Organic Contaminant Oxidation. *Ozone Sci. Eng.* **2011**, *33* (4), 253–266. https://doi.org/10.1080/01919512.2011.578038.

(12) Linge, K. L.; Blair, P.; Busetti, F.; Rodriguez, C.; Heitz, A. Chemicals in Reverse Osmosis-Treated Wastewater: Occurrence, Health Risk, and Contribution to Residual Dissolved Organic Carbon. *J. Water Supply Res. Technol. - AQUA* **2012**, *61* (8), 494–505. https://doi.org/10.2166/aqua.2012.047.

(13) Zeng, T.; Plewa, M. J.; Mitch, W. A. N-Nitrosamines and Halogenated Disinfection Byproducts in U.S. Full Advanced Treatment Trains for Potable Reuse. *Water Res.* **2016**, *101*, 176–186. https://doi.org/10.1016/j.watres.2016.03.062.

(14) Lopachin, R. M.; Gavin, T. Molecular Mechanisms of Aldehyde Toxicity: A Chemical Perspective. *Chem. Res. Toxicol.* **2014**, *27* (7), 1081–1091. https://doi.org/10.1021/tx5001046.

(15) Cho, Y.; Song, M. K.; Kim, T. S.; Ryu, J. C. DNA Methylome Analysis of Saturated Aliphatic Aldehydes in Pulmonary Toxicity. *Sci. Rep.* **2018**, *8* (1), 1–10. https://doi.org/10.1038/s41598-018-28813-z.

(16) Breitner, L. N.; Howe, K. J.; Minakata, D. Effect of Functional Chemistry on the Rejection of Low-Molecular Weight Neutral Organics through Reverse Osmosis Membranes for Potable Reuse. *Environ. Sci. Technol.* **2019**, No. 2, 1DUMMY. https://doi.org/10.1021/acs.est.9b03856.

(17) Agenson, K. O.; Oh, J. I.; Urase, T. Retention of a Wide Variety of Organic Pollutants by Different Nanofiltration/Reverse Osmosis Membranes: Controlling Parameters of Process. *J. Memb. Sci.* **2003**, *225* (1–2), 91–103. https://doi.org/10.1016/j.memsci.2003.08.006.

(18) Xu, P.; Drewes, J. E.; Bellona, C.; Amy, G.; Kim, T.-U.; Adam, M.; Heberer, T. Rejection

of Emerging Organic Micropollutants in Nanofiltration-Reverse Osmosis Membrane Applications. *Water Environ. Res.* **2005**, *77* (1), 40–48. https://doi.org/10.2175/106143005x41609.

(19) Albergamo, V.; Blankert, B.; Cornelissen, E. R.; Hofs, B.; Knibbe, W. J.; van der Meer, W.; de Voogt, P. Removal of Polar Organic Micropollutants by Pilot-Scale Reverse Osmosis Drinking Water Treatment. *Water Res.* **2019**, *148*, 535–545. https://doi.org/10.1016/j.watres.2018.09.029.

(20) Tackaert, R. A.; Pisarenko, A. N.; Chen, E. C.; Kolakovsky, A.; Pecson, B. M.; Drewes, J. E.; Trussell, R. R.; Trussell, R. S. Demonstrating Process Robustness of Potable Reuse Trains during Challenge Testing with Elevated Levels of Acetone, Formaldehyde, NDMA, and 1,4-Dioxane. *J. Water Supply Res. Technol. - AQUA* **2019**, *68* (5), 313–324. https://doi.org/10.2166/aqua.2019.134.

(21) Marron, E. L.; Buren, J. Van; Cuthbertson, A. A.; Darby, E.; Gunten, U. Von; Sedlak, D. L. Reactions of α,β-Unsaturated Carbonyls with Free Chlorine, Free Bromine, and Combined Chlorine. *Environ. Sci. Technol.* **2021**, *55* (5), 3305–3312. https://doi.org/10.1021/acs.est.0c07660.

(22) Kajitvichyanukul, P.; Lu, M. C.; Liao, C. H.; Wirojanagud, W.; Koottatep, T. Degradation and Detoxification of Formaline Wastewater by Advanced Oxidation Processes. *J. Hazard. Mater.* **2006**, *135* (1–3), 337–343. https://doi.org/10.1016/j.jhazmat.2005.11.071.

(23) Marks, R.; Seaman, J.; Perez-Calleja, P.; Kim, J.; Nerenberg, R.; Doudrick, K. Catalytic Hydrogel Membrane Reactor for Treatment of Aqueous Contaminants. *Environ. Sci. Technol.* **2019**, *53* (11), 6492–6500. https://doi.org/10.1021/acs.est.9b01667.

(24) Michael, I.; Frontistis, Z.; Fatta-Kassinos, D. *Removal of Pharmaceuticals from*

Environmentally Relevant Matrices by Advanced Oxidation Processes (AOPs), 2nd ed.; Elsevier B.V., 2013; Vol. 62. https://doi.org/10.1016/B978-0-444-62657-8.00011-2.

(25) Rao, D.; Chen, J.; Dong, H.; Qiao, J.; Zhou, B.; Sun, Y.; Guan, X. Enhanced Oxidation of Organic Contaminants by Mn(VII)/CaSO3 Under Environmentally Relevant Conditions: Performance and Mechanisms. *Water Res.* **2021**, *188*, 116481. https://doi.org/10.1016/j.watres.2020.116481.

(26) Loeb, S. K.; Alvarez, P. J. J.; Brame, J. A.; Cates, E. L.; Choi, W.; Crittenden, J.; Dionysiou, D. D.; Li, Q.; Li-Puma, G.; Quan, X.; Sedlak, D. L.; David Waite, T.; Westerhoff, P.; Kim, J. H. The Technology Horizon for Photocatalytic Water Treatment: Sunrise or Sunset? *Environ. Sci. Technol.* **2019**, *53* (6), 2937–2947. https://doi.org/10.1021/acs.est.8b05041.

(27) Heck, K. N.; Garcia-Segura, S.; Westerhoff, P.; Wong, M. S. Catalytic Converters for Water Treatment. *Acc. Chem. Res.* **2019**, *52* (4), 906–915. https://doi.org/10.1021/acs.accounts.8b00642.

(28) Hurley, K. D.; Shapley, J. R. Efficient Heterogeneous Catalytic Reduction of Perchlorate in Water. *Environ. Sci. Technol.* **2007**, *41* (6), 2044–2049. https://doi.org/10.1021/es0624218.

(29) Chaplin, B. P.; Reinhard, M.; Schneider, W. F.; Schüth, C.; Shapley, J. R.; Strathmann, T. J.; Werth, C. J. Critical Review of Pd-Based Catalytic Treatment of Priority Contaminants in Water. *Environ. Sci. Technol.* **2012**, *46* (7), 3655–3670. https://doi.org/10.1021/es204087q.

(30) Park, J.; An, S.; Jho, E. H.; Bae, S.; Choi, Y.; Choe, J. K. Exploring Reductive Degradation of Fluorinated Pharmaceuticals Using Al2O3-Supported Pt-Group Metallic

Catalysts: Catalytic Reactivity, Reaction Pathways, and Toxicity Assessment. *Water Res.* **2020**, *185*, 116242. https://doi.org/10.1016/j.watres.2020.116242.

(31) Lowry, G. V.; Reinhard, M. Hydrodehalogenation of 1- to 3-Carbon Halogenated Organic Compounds in Water Using a Palladium Catalyst and Hydrogen Gas. *Environ. Sci. Technol.* **1999**, *33* (11), 1905–1910. https://doi.org/10.1021/es980963m.

(32) Zhang, S.; Hedtke, T.; Zhu, Q.; Sun, M.; Weon, S.; Zhao, Y.; Stavitski, E.; Elimelech, M.; Kim, J. H. Membrane-Confined Iron Oxychloride Nanocatalysts for Highly Efficient Heterogeneous Fenton Water Treatment. *Environ. Sci. Technol.* **2021**, *55* (13), 9266–9275. https://doi.org/10.1021/acs.est.1c01391.

(33) Sutherland, A. J.; Ruiz-Caldas, M. X.; de Lannoy, C. F. Electro-Catalytic Microfiltration Membranes Electrochemically Degrade Azo Dyes in Solution. *J. Memb. Sci.* **2020**, *611* (June), 118335. https://doi.org/10.1016/j.memsci.2020.118335.

(34) Zheng, J.; Wang, Z.; Ma, J.; Xu, S.; Wu, Z. Development of an Electrochemical Ceramic Membrane Filtration System for Efficient Contaminant Removal from Waters. *Environ. Sci. Technol.* **2018**, *52* (7), 4117–4126. https://doi.org/10.1021/acs.est.7b06407.

(35) Lee, H.; Lee, H. J.; Seo, J.; Kim, H. E.; Shin, Y. K.; Kim, J. H.; Lee, C. Activation of Oxygen and Hydrogen Peroxide by Copper(II) Coupled with Hydroxylamine for Oxidation of Organic Contaminants. *Environ. Sci. Technol.* **2016**, *50* (15), 8231–8238. https://doi.org/10.1021/acs.est.6b02067.

(36) Zhang, J.; Sun, B.; Guan, X.; Wang, H.; Bao, H.; Huang, Y.; Qiao, J.; Zhou, G. Ruthenium Nanoparticles Supported on CeO2 for Catalytic Permanganate Oxidation of Butylparaben. *Environ. Sci. Technol.* **2013**, *47* (22), 13011–13019. https://doi.org/10.1021/es402118v.

(37) Lee, H.; Kim, H. Il; Weon, S.; Choi, W.; Hwang, Y. S.; Seo, J.; Lee, C.; Kim, J. H. Activation of Persulfates by Graphitized Nanodiamonds for Removal of Organic Compounds. *Environ. Sci. Technol.* **2016**, *50* (18), 10134–10142. https://doi.org/10.1021/acs.est.6b02079.

(38) Weon, S.; Suh, M.-J.; Chu, C.; Huang, D.; Stavitski, E.; Kim, J.-H. Site-Selective Loading of Single-Atom Pt on TiO 2 for Photocatalytic Oxidation and Reductive Hydrodefluorination . *ACS ES&T Eng.* **2021**, *1* (3), 512–522. https://doi.org/10.1021/acsestengg.0c00210.

(39) Zhao, L.; An, H.; Zhao, X.; Wang, Y. TiO2-Catalyzed n-Valeraldehyde Self-Condensation Reaction Mechanism and Kinetics. *ACS Catal.* **2017**, *7* (7), 4451–4461. https://doi.org/10.1021/acscatal.7b00432.

(40) Deng, H.; Li, Z. J.; Wang, X. C.; Wang, L.; Liu, K.; Yuan, L. Y.; Chang, Z. Y.; Gibson, J. K.; Zheng, L. R.; Chai, Z. F.; Shi, W. Q. Efficient Photocatalytic Reduction of Aqueous Perrhenate and Pertechnetate. *Environ. Sci. Technol.* **2019**, *53* (18), 10917–10925. https://doi.org/10.1021/acs.est.9b03199.

(41) Paul, T.; Miller, P. L.; Strathmann, T. J. Visible-Light-Mediated TiO2 Photocatalysis of Fluoroquinolone Antibacterial Agents. *Environ. Sci. Technol.* **2007**, *41* (13), 4720–4727. https://doi.org/10.1021/es070097q.

(42) Hu, L.; Flanders, P. M.; Miller, P. L.; Strathmann, T. J. Oxidation of Sulfamethoxazole and Related Antimicrobial Agents by TiO2 Photocatalysis. *Water Res.* **2007**, *41* (12), 2612–2626. https://doi.org/10.1016/j.watres.2007.02.026.

(43) Richardson, S. D.; Caughran, T. V.; Poiger, T.; Guo, Y.; Gene Crumley, F. Application of DNPH Derivatization with LC/MS to the Identification of Polar Carbonyl Disinfection by-

Products in Drinking Water. *Ozone Sci. Eng.* **2000**, *22* (6), 653–675. https://doi.org/10.1080/01919510009408805.

(44) Rodger B. Baird, Chair Eugene W. Rice, A. D. E. *Standard Methods for the Examination of Water and Wastewater*, 23rd ed.; Water Environment Federation, American Public Health Association , American Water Works Association, 2017.

(45) Dimitrov, S.; Koleva, Y.; Schultz, T. W.; Walker, J. D.; Mekenyan, O. Interspecies Quantitative Structure-Activity Relationship Model for Aldehydes: Aquatic Toxicity. *Environ. Toxicol. Chem.* **2004**, *23* (2), 463–470. https://doi.org/10.1897/02-579.

(46) Cherepakhin, V.; Williams, T. J. Iridium Catalysts for Acceptorless Dehydrogenation of Alcohols to Carboxylic Acids: Scope and Mechanism. *ACS Catal.* **2018**, *8* (5), 3754–3763. https://doi.org/10.1021/acscatal.8b00105.

(47) Appiani, E.; Ossola, R.; Latch, D. E.; Erickson, P. R.; McNeill, K. Aqueous Singlet Oxygen Reaction Kinetics of Furfuryl Alcohol: Effect of Temperature, PH, and Salt Content. *Environ. Sci. Process. Impacts* **2017**, *19* (4), 507–516. https://doi.org/10.1039/c6em00646a.

(48) Keresszegi, C.; Burgi, T.; Mallat, T.; Baiker, A. On the Role of Oxygen in the Liquid-Phase Aerobic Oxidation of Alcohols on Palladium. *J. Catal.* **2002**, *211* (1), 244–251. https://doi.org/10.1006/jcat.2002.3723.

(49) Torres, J. Q.; Royer, S.; Bellat, J. P.; Giraudon, J. M.; Lamonier, J. F. Formaldehyde: Catalytic Oxidation as a Promising Soft Way of Elimination. *ChemSusChem* **2013**, *6* (4), 578–592. https://doi.org/10.1002/cssc.201200809.

(50) Ma, Y.; Zhang, G. Sepiolite Nanofiber-Supported Platinum Nanoparticle Catalysts toward the Catalytic Oxidation of Formaldehyde at Ambient Temperature: Efficient and Stable

Performance and Mechanism. *Chem. Eng. J.* **2016**, *288*, 70–78. https://doi.org/10.1016/j.cej.2015.11.077.

(51) Guo, J.; Lin, C.; Jiang, C.; Zhang, P. Review on Noble Metal-Based Catalysts for Formaldehyde Oxidation at Room Temperature. *Appl. Surf. Sci.* **2019**, *475* (December 2018), 237–255. https://doi.org/10.1016/j.apsusc.2018.12.238.

(52) Ye, J.; Zhu, B.; Cheng, B.; Jiang, C.; Wageh, S.; Al-Ghamdi, A. A.; Yu, J. Synergy between Platinum and Gold Nanoparticles in Oxygen Activation for Enhanced Room-Temperature Formaldehyde Oxidation. *Adv. Funct. Mater.* **2022**, *32* (15), 1–10. https://doi.org/10.1002/adfm.202110423.

(53) Doussin, J. F.; Monod, A. Structure-Activity Relationship for the Estimation of OH-Oxidation Rate Constants of Carbonyl Compounds in the Aqueous Phase. *Atmos. Chem. Phys.* **2013**, *13* (23), 11625–11641. https://doi.org/10.5194/acp-13-11625-2013.

(54) Winstein, S.; Lucas, H. J. The Hydration of Unsaturated Compounds. VI. The Rate of Hydration of Trans-Crotonaldehyde. The Equilibrium between Trans-Crotonaldehyde and Aldol in Dilute Aqueous Solution. *J. Am. Chem. Soc.* **1937**, *59* (8), 1461–1465. https://doi.org/10.1021/ja01287a015.

(55) Thus, H.; Mcclelland, R. A.; Coe, M. Structure-Reactivity Effects in the Hydration of Benzaldehydes. **1983**, *11* (4), 4005–4012.

(56) Grunwaldt, J. D.; Caravati, M.; Baiker, A. Oxidic or Metallic Palladium: Which Is the Active Phase in Pd-Catalyzed Aerobic Alcohol Oxidation? *J. Phys. Chem. B* **2006**, *110* (51), 25586–25589. https://doi.org/10.1021/jp066949a.

(57) Iwasa, N.; Takezawa, N. New Supported Pd and Pt Alloy Catalysts for Steam Reforming and Dehydrogenation of Methanol. *Top. Catal.* **2003**, *22* (3–4), 215–224.

https://doi.org/10.1023/A:1023571819211.

(58) Mallat, T.; Baiker, A. Catalyst Potential: A Key for Controlling Alcohol Oxidation in Multiphase Reactors. *Catal. Today* **1995**, *24* (1–2), 143–150. https://doi.org/10.1016/0920-5861(95)00016-9.

(59) Cherepakhin, V.; Williams, T. J. Direct Oxidation of Primary Alcohols to Carboxylic Acids. *Synth.* **2021**, *53* (6), 1023–1034. https://doi.org/10.1055/s-0040-1706102.

(60) Williams, T. J.; Kershaw, A. D.; Li, V.; Wu, X. An Inversion Recovery NMR Kinetics Experiment. *J. Chem. Educ.* **2011**, *88* (5), 665–669. https://doi.org/10.1021/ed1006822.

(61) Eric V. Anslyn and Dennis A. Dougherty. *Modern Physical Organic Chemistry*; University science books, 2006.

(62) Wang, X. X.; Zheng, H. Y.; Liu, X. J.; Xie, G. Q.; Lu, J. Q.; Jin, L. Y.; Luo, M. F. Effects of NaCl on Pt/ZrO2 Catalysts for Selective Hydrogenation of Crotonaldehyde. *Appl. Catal. A Gen.* **2010**, *388* (1–2), 134–140. https://doi.org/10.1016/j.apcata.2010.08.044.